Characterization of antibiofouling behaviors of PVDF membrane modified by quaternary ammonium compound – combined use of QCM-D, FCM, and CLSM

Yue Wen, Xingran Zhang, Mei Chen, Zhichao Wu and Zhiwei Wang

ABSTRACT

In this study, we systematically evaluated the antibiofouling behavior of quaternary ammonium compound (QAC) blended polyvinylidene fluoride (PVDF) membrane using quartz crystal microbalance with dissipation monitoring (QCM-D) combined with flow cytometry (FCM) and confocal laser scanning microscopy (CLSM) measurements. QCM-D tests showed that the introduction of QAC reduced bacterial attachment due to the biocidal functions of QAC. FCM indicated that cell integrity of the bacteria in the suspension flowing along QAC-modified membrane surfaces during the QCM-D test was severely affected. CLSM confirmed the significantly lower attachment of bacteria and higher dead/live cell ratio onto the surface of modified membranes after the washing step in QCM-D tests. Both FCM and CLSM results validated the antibacterial behavior of QAC-modified membranes by a contact-killing mechanism, which is in agreement with that of QCM-D tests. In addition, the bacterial cells accumulated on modified membrane surface exhibited higher reversibility compared to the control membrane, indicating ease of membrane cleaning. The results highlight that the combined use of QCM-D, FCM, and CLSM can comprehensively characterize the antibiofouling behavior of membranes.

Key words | antibiofouling, contact-killing mechanism, membrane modification, polyvinylidene fluoride (PVDF) membrane, wastewater treatment

Yue Wen
Xingran Zhang
Mei Chen
Zhichao Wu
Zhiwei Wang (corresponding author)
State Key Laboratory of Pollution Control and Resource Reuse, Shanghai Institute of Pollution Control and Ecological Safety, School of Environmental Science and Engineering,
Tongji University,
1239 Siping Road, Shanghai 200092,
China
E-mail: *zwwang@tongji.edu.cn*

INTRODUCTION

Membrane fouling, particularly biofouling, is a critical issue, in commonly used membrane-based technologies for water and wastewater treatment, and increases the overall treatment cost as a result of frequent membrane cleaning and replacement (Oh *et al.* 2012; Venault *et al.* 2016). Development of antibiofouling membranes via surface modification is an efficacious strategy in curbing membrane fouling. To date, surface modification of membranes involves functionalization with releasable bacteria-killing substances (termed release-killing), such as silver nanoparticles (Rahaman *et al.* 2014; Ye *et al.* 2015), magnetic nanoparticles (Durmus *et al.* 2013), and triclosan (Makarovsky *et al.* 2011), or modification with bactericidal materials such as graphene oxide (Perreault *et al.* 2014), photoactive agents (Mollahosseini & Rahimpour 2014), and antibiotics (Blok *et al.* 2014) for contact-killing. Compared to release-killing protocols, contact-killing is more effective since antimicrobial agents on the membrane surfaces have higher structural stability and lower partial blocking of surface pores (Shannon *et al.* 2008; Venault *et al.* 2014).

doi: 10.2166/wrd.2018.017

Quaternary ammonium compounds (QACs) are a kind of antimicrobial agents (Hu *et al.* 2016), which contain a long hydrophobic alkyl chain covalently attached to a central nitrogen atom (NR_4^+). QACs exhibit good antimicrobial activity by inducing an interaction with cell membranes, disruption of cell membrane integrity, and consequent leakage of cellular content (Tezel & Pavlostathis 2015). QACs have been used for coating/preparing a variety of antimicrobial surfaces (Fadida *et al.* 2014; Zhang *et al.* 2014), and incorporation of QACs into polymeric membranes can give then antibacterial properties (Tiraferri *et al.* 2012; Ye *et al.* 2015; Zhang *et al.* 2016a, 2016b). Clarification of the interfacial behavior of bacterial attachment is of great importance for understanding antibiofouling mechanisms (Tagaya *et al.* 2011) and can further facilitate design of superior antibiofouling membranes.

Available techniques including quartz crystal microbalance with dissipation monitoring (QCM-D), flow cytometry (FCM), and confocal laser scanning microscopy (CLSM) (Kuyukina *et al.* 2014; Olsson *et al.* 2015) show great potential for characterizing fouling behavior and the existing status of microbial cells on surfaces. QCM-D provides real-time information on microbial attachment on membranes by using membrane-coated sensors (Lord *et al.* 2008; Contreras *et al.* 2011; Goda & Miyahara 2012; Chowdhury *et al.* 2014). CLSM can be used to detect the live/dead cells attached to membrane surfaces (Zhang *et al.* 2015a, 2015b), and FCM, coupled with staining techniques, can show changes in cell integrity (Habtewold *et al.* 2016). Although the above-mentioned techniques can be separately used for characterizing the interfacial behavior, their combined use is necessary to provide a more comprehensive understanding of biofouling/antibiofouling behavior.

The objective of this study is to investigate the antibacterial performance and associated mechanism of an antibiofouling membrane, i.e., QAC-modified polyvinylidene fluoride (PVDF) membrane, via the combined use of QCM-D, CLSM, and FCM. Bacterial attachment was monitored using QCM-D, with live/dead conditions on membrane surfaces examined by CLSM and in the elution flowing along QAC-modified membrane surfaces by FCM. The biofouling structural information (elasticity/rigidity) together with its reversibility on the interface was also analyzed.

MATERIALS AND METHODS

Chemicals and reagents

Commercial grade PVDF was purchased from Solvay Corporation with M_W in the range 670–700 kDa. Dimethyl sulfoxide (DMSO) was used as a solvent and polyethylene glycol (PEG 600, analytical reagent) used as a pore-forming additive, which were both purchased from Sinopharm (Shanghai, China). Dodecyl dimethyl benzyl ammonium chloride (DDBAC, a type of QAC), purchased from Sigma-Aldrich, was used in this study. Gram-negative *Escherichia coli* (*E. coli*, ATCC25922) suspensions (Shanghai Weike Biotechnology Corporation) were prepared by dispersing the colonies from agar slants in sterile saline. *E. coli* was chosen for this study because it is widely found in the environment (Liu *et al.* 2014) and has been used frequently as a model organism to characterize antibacterial behavior and to investigate the performance of disinfectants, antiseptics, and antibiofouling materials (Li *et al.* 2006, 2016; Yang *et al.* 2016). Unless specified otherwise, all chemicals were of analytical grade. Sodium chloride and *n*-dodecane were purchased from Aladdin (China). Deionized (DI) water was used throughout all experiments.

QAC-blended PVDF casting solution

The membranes used in this study were prepared by the phase inversion method as described in our previous publication (Zhang *et al.* 2015a, 2015b). Blending is the simplest and most widely used method to modify polymeric membranes. The modified membranes are stable, and additives are scarcely leached (Liu *et al.* 2011). A predetermined amount of PVDF (8.0 wt%) and PEG (8.0 wt%), after drying for 24 h at 80 °C to eliminate moisture, was dissolved in DMSO, followed by agitation at 80 °C for 48 h to obtain a homogeneous solution. A QAC solution was prepared by dissolving a predetermined amount of DDBAC (0.0, 0.1, 0.2, and 0.4 wt%) in DMSO. The two solutions were then mixed and stirred at 80 °C for 32 h prior to degassing with ultrasonication for at least 0.5 h. The casting solution can be used for preparing membranes or for coating the crystal sensors of QCM-D. The modified membranes made from

the casting solutions or the coated crystal sensors with 0.1, 0.2, and 0.4 wt% QAC were identified as Q0.1, Q0.2, and Q0.4, respectively. The pristine PVDF membrane or the coated crystal sensor using PVDF casting solution without QAC was termed Q0. Our previous study (Zhang *et al.* 2016a, 2016b) showed that less than 10% of antibacterial activity were caused by the leaching of QACs at the beginning of the experiments.

Membrane characterization

Surface hydrophilicity of the membranes was determined by the sessile drop contact angle (CA) method (OCA 15 Plus, Data Physics GmbH, Germany) (Qi *et al.* 2015). Zeta potential of the membrane surface was determined at a solution ionic strength of 10 mM KCl and a pH value of 7 by a streaming potential analyzer (EKA 1.00, Anton- Paar, Swiss) (Zhang *et al.* 2016a, 2016b). The pH value of 7 was chosen because water and wastewater are always circumneutral (Wang *et al.* 2016). At least three measurements were conducted for each sample. The presence of QAC on membranes was evaluated by attenuated total reflectance Fourier-transform infrared spectroscopy (FTIR) on a Nicolet 6700 (Thermo Fisher, America). Membrane morphologies were observed by a field emission scanning electron microscope (SEM, SU8010, Hitachi, Japan) (Dong *et al.* 2013), with surface pore sizes of membranes calculated by the Image-pro plus 6.0 software (Media Cybernetics, USA).

Preparation of bacterial suspension

Twenty microliters of adjusted bacterial suspension (about 10^7 cells mL^{-1}) was poured into a 12-well plate with 20 mL nutrient broth (Sinopharm). Subsequently, the bacterial cultures were incubated in the dark on a rotary shaker (100 rpm) at 37 °C overnight. Bacteria were harvested by centrifugation (at 4,000 *g* and 4 °C for 10 min) and washed three times with sterile saline, excluding the influence of residual substrate on the interaction of bacteria and membrane surface and ensuring all bacteria were in the same growth phase. After harvesting and washing, the bacterial suspension was adjusted via dilution to an optical density (OD_{600}) measured by a spectrophotometer (TU-1810, PERSEE, China) equal to 1, which corresponded to $5 \times 10^8 \pm 5 \times 10^6$ cells/mL. The adjusted bacterial suspensions were used for all subsequent experiments (Gutman *et al.* 2013).

Bacterial characterization

The zeta potential of *E. coli* suspensions was measured by a zeta potential analyzer (Zetasizer Nano Z9, Malvern Instruments Ltd., UK) at an OD = 1. Experiments were conducted at pH of 7 and temperature of 25 °C at least three times (Gutman *et al.* 2013).

The MATH (microbial adherence to hydrocarbons) method (Pembrey *et al.* 1999) was used to measure bacterial hydrophobicity and to ensure similar surface hydrophilicity of cells used in tests. Bacterial suspensions were adjusted to a predetermined concentration with an OD_{600} equal to 0.3, and 4 mL suspensions were then transferred into test tubes containing 1 mL n-dodecane. The test tubes were vortexed for 2 min, followed by phase separation for 45 min. The OD_{600} of the cells in the aqueous phase was measured to determine the quantity of bacterial cells partitioning between the n-dodecane and the bulk solution. Sterile saline was used as a control. The tests were repeated three times. Hydrophobicity is reported as the ratio of cells partitioned into the hydrocarbon to total cells.

Membrane fouling analysis

Cell attachment analysis using QCM-D

QCM-D (Q-sense AB, Gothenburg, Sweden), which employs an ultrasensitive coin-shaped quartz sensor housed inside a flow cell with a well-defined geometry and hydrodynamic characteristics, was used to study the biofouling behavior of QAC-modified membrane (Marcus *et al.* 2012). When bacteria attach to the surface, the total oscillating mass increases, which results in a decrease in the frequency and an increase in the energy dissipation. The quantity of deposited bacteria is proportional to the frequency shifts (Δf, Hz) (Olofsson *et al.* 2005; Gutman *et al.* 2013).

Quartz crystals (QSX301, Q-sense) were coated with different membrane recipes by a spin coater (KW-4A, Chemat, China) (Zhang *et al.* 2015a, 2015b). Casting solutions were diluted 20-fold in DMSO. The diluted casting solution

was dropped onto the quartz crystal for 15 s at a spinning rate of 1,500 rpm, and then followed by 30 s at a spinning rate of 6,000 rpm based on our preliminary study. The coated quartz crystals were evaporated at 80 °C for 2 h. All QCM-D experiments were performed under flow-through conditions using a digital peristaltic pump (IsmaTec Peristaltic pump, IDEX) with a flowrate 150 μL/min. Different solutions were injected sequentially to the QCM-D system: (A) deionized water for 10 min; (B) sterile saline background solutions for 10 min; (C) suspended bacteria in the background solution at $OD_{600} = 0.1 \pm 0.01$ ($5 \times 10^7 \pm 5 \times 10^6$ cells·mL^{-1}) for 1 h; (D) sterile saline background solutions for 20 min; and (E) deionized water for 20 min. Each experiment was repeated to ensure the reproducibility of the results (Zhang *et al.* 2015a, 2015b). The variations of the changes in frequency (Δf, Hz) and dissipation factors (ΔD) were monitored at the third overtone. Initial deposition rate (r_f) is defined as rate of frequency shift in a time period t (Gutman *et al.* 2013):

$$r_f = \left| \left(\frac{\mathrm{d}\Delta f}{\mathrm{d}_t} \right)_{t \to 0} \right| \quad (1)$$

The reversible and irreversible properties of attached bacteria on membranes were evaluated based on the removed fraction and unremoved fraction in the washing phase using DI water (stage E), which can be shown by the percentages of Δf changed after washing. In detail, the relative Δf of reversible fouling (Δf_{rev}) and irreversible fouling (Δf_{irr}). were calculated by Equations (2) and (3), respectively.

$$\Delta f_{rev} = 1 - \frac{|\Delta f_E - \Delta f_B|}{|\Delta f_D|} \quad (2)$$

$$\Delta f_{irr} = \frac{|\Delta f_E - \Delta f_B|}{|\Delta f_D|} \quad (3)$$

where Δf_B is the stable Δf after sterile saline background solution injection in stage B, Δf_D is the stable Δf at the end of bacterial attachment in stage D, and Δf_E is the stable Δf after DI water washing in stage E.

Representative normalized frequency (Δf) shifts at the third overtone on various casting solution coated quartz crystals are shown in SI Figure S1. In stage A, DI water was injected to attain a stable baseline. Sterile saline background solution was injected subsequently in stage B. During the injection of bacterial suspension, Δf decreased sharply (stage C), suggesting the attachment of bacteria onto the sensors. In stage D, background sterile saline solution was introduced, followed by a DI water rinse in the final stage (stage E), and the change of frequency shift during DI water rinse indicated desorption of the bacteria from the sensors.

Extended Derjaguin-Landau-Verwey-Overbeek (XDLVO) theory was used to illustrate the interaction behavior between the membrane surface and foulants at the initial stage of biofouling (Thwala *et al.* 2013; Feng *et al.* 2014). Although XDLVO theory cannot be used to predict bacterial adhesion directly, it may disclose the physicochemical changes of the bacteria and sensor surfaces that impact cell deposition (Vanoyan *et al.* 2010). Surface tensions for membranes and foulants were calculated according to literature (Zhang *et al.* 2016a, 2016b). Details about the calculation process can be found in SI Section S1.

Live/dead cell staining and FCM analysis

During QCM-D experiment, bacterial suspension effluents were collected and diluted with DI water, and followed by staining with the LIVE/DEAD® BacLight™ Bacterial Viability Kit L7012. The nucleic acid stain SYTO 9 stains live cells, and propidium iodide (PI) stains dead cells. SYTO 9 and PI were added to final concentrations of 3 μM and 20 μM, respectively, from a stock solution in DMSO according to manufacturer's instructions. The mixture was incubated for 15 min in the dark. FCM (BD FACSVerse, BD Biosciences, USA) was used for examining cell integrity at a flow rate of 10 μL/min. Fluorescence emission for the cells stained with SYTO 9 and PI were detected at 530 nm and 576 nm, respectively (Khan *et al.* 2010).

CLSM analysis

After the QCM-D tests, the sensors were removed and gently washed with DI water. The adherent bacteria on the sensors were stained with the LIVE/DEAD® BacLight™ Bacterial Viability Kit L7012. According to manufacturer's instructions, SYTO 9 (final concentration of 3 μM) and PI (final concentration of 20 μM) were diluted using DI water. The

sensors were covered with staining solution and incubated for 15 min in the dark, and then washed again with DI water. The bacterial distribution on the sensors was analyzed by using a Leica TCS SP5 II confocal microscope (Wetzlar, Germany) with a plan-apochromat, oil immersion 63×, 1.4 numerical aperture lens with the filter sets SYTO 9 (BP 450–490, FT 510, BP 515–565) and PI (BP 546/612, FT 580, LP 590). Images were captured at a scanning speed of 200 Hz and image resolution of 1,024 × 1,024 pixels, and subsequently analyzed using Leica Application Suite 1.31 (Pires *et al.* 2013). At least 10 fields of view were measured for each surface. Image analysis was performed using Image J software (http://rsbweb.nih.gov).

RESULTS AND DISCUSSION

Membrane characterization

Table 1 shows the intrinsic characteristics of pristine and modified membranes. The physicochemical characteristics were slightly changed due to the successful presence of QAC on the membrane surfaces. Membrane hydrophilicity was mildly decreased with the increase of QAC dosage, whereas membrane surface charge became less negative (Dai *et al.* 2016). The decrease of hydrophilicity of the membrane surface may be attributed to the alkyl chains of QAC (Harney *et al.* 2009), while the decrease of negative zeta potential may be due to positively charged nitrogen atoms from QAC. *E.coli* has negatively charged zeta potentials (pH = 7) of −18.9 ± 0.4 mV due to the presence of anionic surface groups, such as carboxyl and phosphate (Thwala *et al.* 2013), which suggest the decrease of membrane negative zeta potential may increase the interactions between bacteria and membranes. The FTIR spectra of Q0, Q0.1, Q0.2, and Q0.4 are shown in SI Figure S2. Three strong characteristic peaks at 879, 1,174, and 1,400 cm^{-1}, ascribed to skeletal vibration of PVDF C-C bonds, -CF_2- stretching, and -CH_2- in plane blending, respectively, are observed in all spectra (Zhu *et al.* 2017). The peak at ~1,664 cm^{-1} can be assigned to C = O stretching and C-N stretching (Wadekar & Vidic 2017), which increased significantly as the QAC dosage increased compared to the pristine membrane, suggesting a successful introduction of C-N groups of QAC into membrane matrix. Unmodified membrane Q0 also had the peak at 1,664 cm^{-1}, which was mainly due to the residual PEG (additive) on the membrane surface since PEG contains oxygen atoms. SI Figure S3 shows the surface morphologies of these four membranes. All the membranes had a porous layer. Pore size became larger when the concentration of QAC in the dope solution increased from 0 to 0.2 wt% ($p < 0.05$). After the QAC content reached 0.4 wt%, the average pore size decreased ($p < 0.05$). DDBAC is an amphiphilic surfactant, containing both hydrophilic heads and hydrophobic tails. The increase of dosage leads to an accumulation of its hydrophilic heads in the polymer structure and thus an enhanced repulsion between polymer chains (a larger pore size). However, the further increase of dosage may result in the formation of QAC micelles (with polar groups on the outer surface and non-polar groups inside the micelles). As a result, the pore sizes of modified membranes decreases (Hu *et al.* 2016).

Table 1 | Characterization of the control membrane Q0 and QAC-blended membranes, Q0.1 (0.1 wt %), Q0.2 (0.2 wt %), and Q0.4 (0.4 wt %)

Membranes	Surface contact angle (°)	Surface charge (mV)	Average pore size (nm)
Q0	54.3 ± 3.1	−14.5 ± 0.8	79.9 ± 21.6
Q0.1	63.5 ± 0.2	−6.3 ± 1.2	85.2 ± 25.9
Q0.2	65.9 ± 1.7	−5.7 ± 3.2	138.6 ± 68.8
Q0.4	67.7 ± 2.2	−3.0 ± 1.4	93.1 ± 28.7

Antibacterial behavior

Anti-attachment behavior

QCM-D measurement is an effective method to investigate the dynamic adsorption processes at a solid/liquid interface. In this study, frequency shift of the sensors was used to indicate the quantity of bacteria attached to the sensors. The values of Δf at the end of the bacterial attachment phase are shown in Figure 1. The result showed that bacterial attachment was reduced significantly ($p < 0.05$) for QAC/PVDF solution coated sensors compared to the pristine one, exhibiting excellent resistance to the adsorption of bacteria. The effective antibacterial activity of QAC is consistent with the literature reporting material surface coatings using

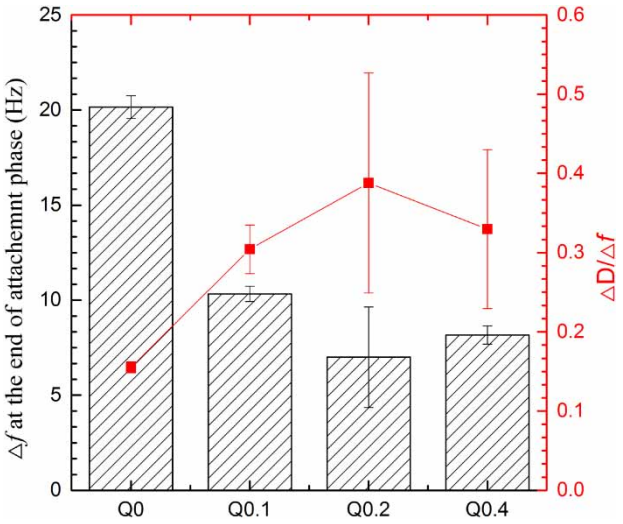

Figure 1 | Change of frequency (Δf) and $|\Delta D/\Delta f|$ values at the end of bacterial attachment phase and for Q0, Q0.1, Q0.2, and Q0.4 coated quartz crystals sensors. Error bars represent standard deviations of at least three runs.

QAC (Gerba 2015; Tezel & Pavlostathis 2015; Zhang *et al.* 2016a, 2016b). Q0.4 with a higher dosage did not show a lowered adsorption compared to Q0.2, suggesting that 0.2% might be an optimal QAC concentration for membrane preparation since the increase in QAC dosage might induce the deterioration in membrane intrinsic properties, compromising the antibiofouling behavior. As shown in Table 1, the larger dosage of QAC affected membrane hydrophilicity and negative surface charge due to its long alkyl chain and positive N^+ group, which would cause more intensive physicochemical interactions between membranes and foulants based on XDLVO theory. With the increase of QAC dosage, the effect of physicochemical interaction might be larger than that of the physiological interaction, leading to the limited antibiofouling behavior.

In addition, the $|\Delta D/\Delta f|$ value can be used to analyze structural information about the adsorbed layer (Contreras *et al.* 2011). A rigid adsorption layer has a low $|\Delta D/\Delta f|$ value, while an elastic layer is accompanied with a large $|\Delta D/\Delta f|$ value (Olsson *et al.* 2010). $|\Delta D/\Delta f|$ values (Figure 1) showed that the adsorbed layer of Q0.1, Q0.2, and Q0.4 coated crystal surfaces were more fluid and elastic, while Q0 had the significantly rigid adsorbed layer at the end of bacterial attachment phase ($p < 0.05$). This implies that the interactions between bacteria and QAC-blended membranes were impaired compared to pristine ones (Olofsson *et al.* 2005). The rigidity of the adsorption layer on Q0 might be due to the largest mass adsorption, which gradually compressed the adsorbed layer (Lu *et al.* 2013). The increased rigidity of the adsorption layer indicate an irreversible and gradually matured cell attachment, facilitating subsequent biofilm formation on the membrane surface (Schofield *et al.* 2007). In contrast, the killed bacteria on modified surfaces became loosely bound to the surface. This is mainly due to the fact that when the bacteria were damaged, the interaction of cell with membrane surface necessary for irreversible attachment might be inhibited due to the decreased production of curli and adhesion molecules, which would lead to their detachment from the membrane surface (Hori & Matsumoto 2010). Therefore, the elastic properties of the fouling layers on Q0.1, Q0.2, and Q0.4 sensors increased (Ronen *et al.* 2015). Additionally, the affected microbes might be also capable of causing feedback, similar to quorum sensing, to reduce bacterial deposition and attachment (Vanoyan *et al.* 2010). The feedback, such as inhibition of respiratory enzymes and dissipation of the proton motive force, is likely to trigger an SOS response via cell regulation or signaling (Ceragioli *et al.* 2010; Tezel & Pavlostathis 2011), thus inhibiting the attachment of bacteria in the vicinity.

To further confirm the antibiofouling behavior of membranes, the initial attachment rates were determined based on the initial slope of Δf (Chowdhury *et al.* 2014). As shown in Figure 2, the pristine PVDF-coated sensor (Q0) shows the greatest rate of cell attachment on the sensor; however, the QAC-modified membranes exhibit significantly lower attachment rate compared to Q0 ($p < 0.05$). The results indicated the pristine PVDF-coated sensor (Q0) was more favorable for *E. coli* attachment which cannot be explained by physicochemical interactions between *E. coli* and membrane, since Q0 had the lowest contact angle and highest negative zeta potential.

XDLVO theory was further used in this study to quantify physicochemical interaction energies between foulants and membrane surfaces. According to XDLVO theory, the attachment of bacteria onto a surface is governed by van der Waals attraction forces, electrostatic forces, and acid-base interactions (Hermansson 1999; Kang *et al.* 2004;

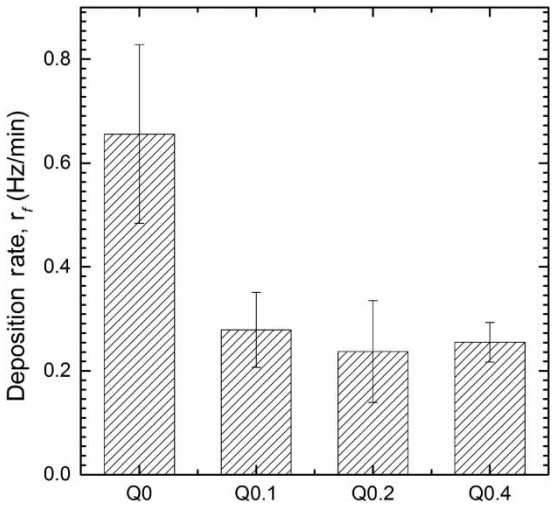

Figure 2 | Initial adsorption rate of *E. coli* for Q0, Q0.1, Q0.2, and Q0.4 coated quartz crystals sensors. Error bars represent standard deviations of at least three runs.

Ronen *et al.* 2015). Based on the calculation, QAC-modified membranes would have a stronger adhesion potential (see SI Figure S4) compared to the control. However, the QCM-D results are inconsistent with the XDLVO prediction. It might be due to the fact that the attachment behavior of bacteria was significantly altered by the introduction of QAC (Gao *et al.* 2016). Once the microbes are in contact with QAC, contact-killing begins to dominate the interaction. On the other hand, surface charge heterogeneity induced by QAC might also affect the prediction (Vanoyan *et al.* 2010). It shows that the antibiofouling membrane surface has its special interaction with bacteria due to the contact-killing effects (Vadillo-Rodríguez & Logan 2006; Vanoyan *et al.* 2010). The difference between the XDLVO theory and research results may be associated with physiological changes attributed to the introduction of the antimicrobials QAC into membranes.

In summary, bacteria adsorption equilibrium data suggests that the contact-killing mechanism induced by QAC plays an important role in bacterial adsorption in addition to the nonspecific electrostatic and hydrophobic interactions. Therefore, water contact angle and surface zeta potential are not good indicators for bacterial adsorption. Membranes with less negative zeta potential and large contact angle due to the presence of QAC may be less prone to bacterial fouling.

CLSM and FCM measurements

In order to characterize the bactericidal behavior of QAC-blended membrane, FCM was used to evaluate cell integrity of the bacterial suspension efflux during the adsorption phase in the QCM-D experiment (stage C in SI Figure S1), and the results are presented in Figure 3. The ratio of dead cells (broken cells) to live cells (intact cells) increased with the increase of QAC dosage, indicating that the modified membrane could efficiently kill microorganisms. According to antibacterial tests of our previous study, the antibacterial efficiency of QAC-modified membrane reached a stable value after immersion in water for 4 h, indicating that the antibacterial efficiency of QAC-modified membrane could last for a long time. In this process, contact killing dominated the antibacterial behavior (Zhang *et al.* 2016a, 2016b). The slight increase of dead/live ratios in the elution of QCM-D experiment suggested only a small proportion of bacteria that contacted the QAC-modified sensors were killed although a large number of bacteria flowed through the QCM-D system. Therefore, the FCM results confirmed that contact-killing rather than release-killing played an important role in the adsorption of bacteria onto QAC-modified membrane. The bactericidal behavior might involve two mechanisms: (i) the replacement of bacterial counter ions

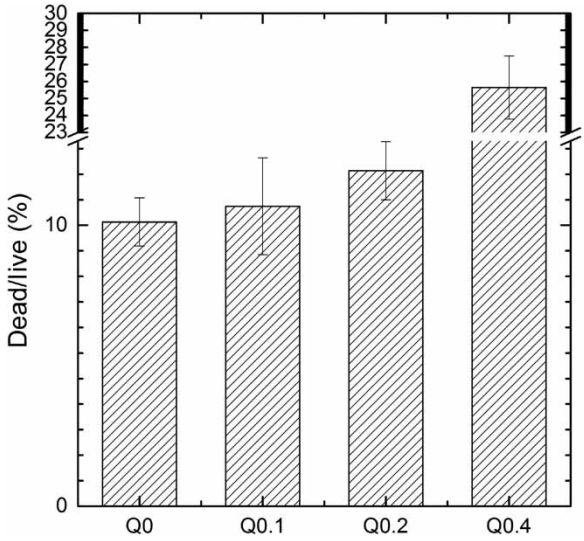

Figure 3 | Dead/live cell ratio on sensors revealed by FCM. The parameters were calculated by FlowJo 7.6.1. Error bars represent standard deviations of at least three runs.

(Mg^{2+} and Ca^{2+}), which are initially confined within the cell membrane, by positively charged polyatomic ions of the structure NR_4^+, thus disrupting the ionic integrity of the membrane (Kügler *et al.* 2005; Gao *et al.* 2016); (ii) the penetration of alkyl chains into the phospholipid bilayer structure which causes defects in the cell membrane, destroying the cell integrity (Gao *et al.* 2016; Hu *et al.* 2016).

CLSM was utilized to further examine the existing status of bacteria adsorbed onto the sensors at the end of the QCM-D experiments (Figure 4). For Q0, *E. coli* could be observed with abundant viable bacteria covering the sensor surface. In contrast, in the presence of QAC, the total *E. coli* cells decreased significantly, exhibiting evidently antibiofouling behavior. The results suggest that attachment of cells to membrane surface can be greatly decreased by cell deactivation as well as cell death (Liu *et al.* 2013). To further verify the bactericidal effects of QAC-modified membrane, the ratio of dead cells to live cells for pristine and modified membranes is shown in Figure 5. It is evident that with the increase of QAC dosage, the dead/live cell ratio on membrane surfaces increased ($p < 0.05$ for Q0.4). The results are also consistent with FCM tests for cells in the eluate, clearly demonstrating the antibacterial behavior of the QAC-modified membrane.

In our previous study (Chen *et al.* 2017), the antibiofouling performance, mechanisms, and effects on bacterial community of QAC-modified membrane were systematically evaluated in an membrane bioreactors for treating real municipal wastewater. The result indicated that QAC-modified PVDF membranes could retard the development of cohesive biofilm through killing bacteria attached to their surface and only allow organic matter with strong adhesion

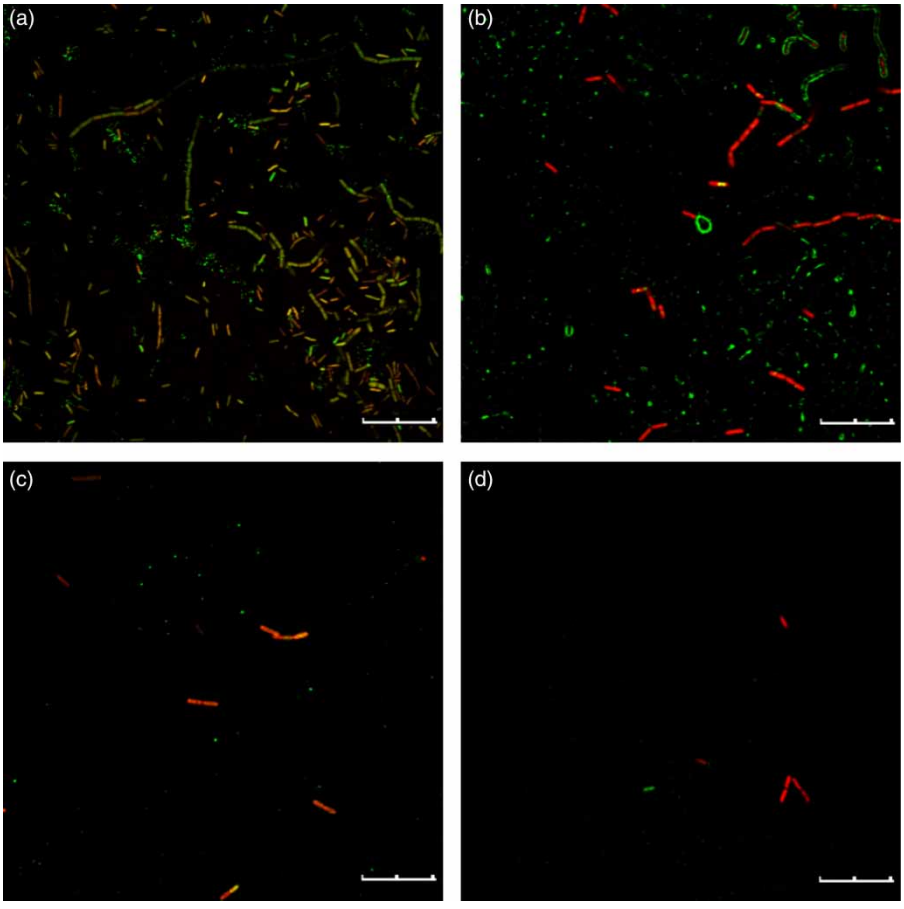

Figure 4 | CLSM images of all the membranes after QCM-D experiments. (a–d) are the surface images of Q0–Q0.4, respectively. The live (stained green) and dead cells (stained red) on the sensors were stained with the LIVE/DEAD® BacLight™ Bacterial Viability Kit L7012. Scale bars = 20 μm.

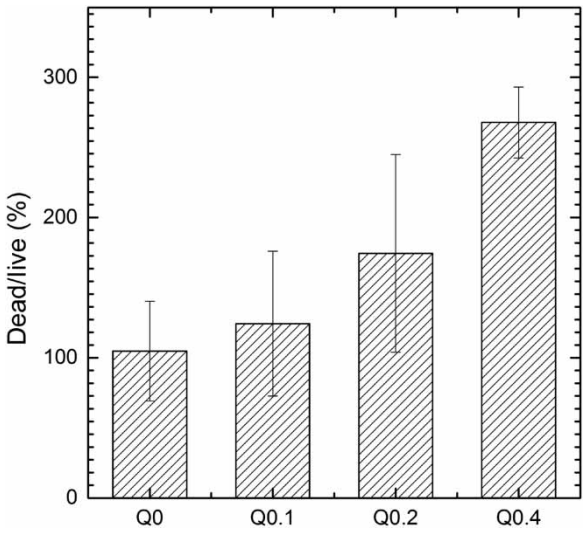

Figure 5 | Dead/live cell ratio on sensors revealed by CLSM. The parameters were calculated from CLSM images. Error bars represent standard deviations of at least three fields of view for each surface.

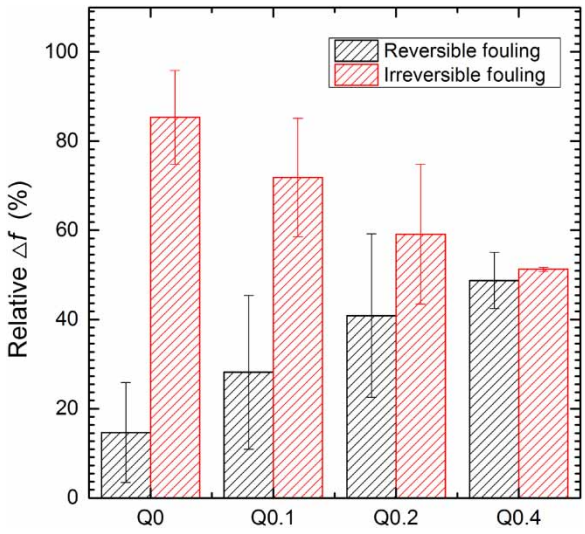

Figure 6 | Relative Δf of adsorbed bacteria on Q0, Q0.1, Q0.2, and Q0.4 sensors after introducing DI water (i.e., reversible fouling and irreversible fouling), respectively. Error bars represent standard deviations of at least three runs.

properties to remain on the membrane surface. It suggests that the QAC-modified membranes also have antifouling efficiencies in real applications.

Reversibility of the adsorbed bacteria

In the design of antibiofouling membranes, it is very important to consider both initial bacterial adhesion and the ease of cleaning after killing. Therefore, the reversibility of membrane foulants was further investigated, with results shown in Figure 6 based on the frequency shifts before/after introducing DI water. It can be observed that the reversible fouling proportion of QAC-modified membranes was significantly higher than that of the pristine membrane ($p < 0.05$). This is also supported by the fluidity of the adsorbed bacteria on membrane surfaces ($|\Delta D/\Delta f|$). These results suggest that the bacteria affected via contact-killing effects might not firmly attach to the QAC-modified membrane, leading to ease of cleaning. Such effect could also partially explain why the QAC-modified membrane had lower adsorption mass.

The antibacterial mechanisms of QAC-blended membrane are further illustrated in Figure 7. For pristine membrane, the fouling behavior is dependent on physiochemical interaction between bacteria and membrane, exhibiting larger bacteria deposition and lower reversibility.

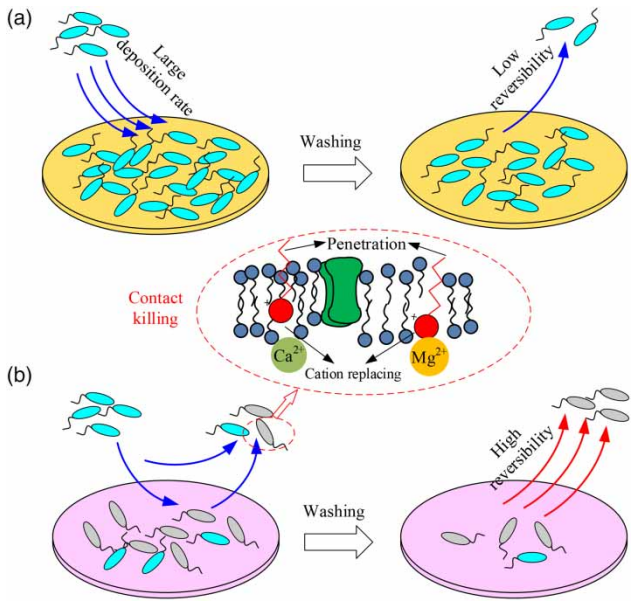

Figure 7 | Schematic representation of the possible antibacterial mechanisms for pristine and modified membranes. (a) Pristine membrane; (b) modified membrane.

For QAC-modified membrane, the interaction between membrane and bacteria cannot be simulated well by the XDLVO theory, which might be due to the change of heterogeneity of surface charge induced by QAC and, more importantly, contact-killing effects. The physiological interaction between QAC-modified membrane and bacteria resulted in the lower quantity of deposited bacterial mass,

higher fluidity of biofouling layer, and slower initial deposition rate (Figures 1 and 2). The divalent cations, such as Mg^{2+} and Ca^{2+}, present on the outermost membrane surface, are able to stabilize bacterial membranes; however, the positively charged QAC may attach to the polar surface by replacing Mg^{2+}/Ca^{2+}. This will facilitate the penetration of the hydrophobic alkyl chain into the phospholipid bilayer, causing the death of microbial cells (Gilbert & Moore 2005; Dolezal *et al.* 2016). The contact-killing effects also led to the looser attachment of bacteria to membrane surfaces and higher reversibility (Figures 1 and 6). Additionally, the affected bacteria on QAC-modified membrane could also possibly induce the production of some signals (Blango & Mulvey 2009) for cells in the vicinity to escape from the surface, thus limiting the attachment of bacteria. In addition, since many bacteria have extracellular polymeric substances that could affect the interaction between cell and membrane surface; the role of extracellular polymeric substances in cell attachment needs further investigation.

CONCLUSIONS

In this study, DDBAC, a type of QAC was introduced into PVDF membrane, and its antibiofouling behavior was systematically investigated using QCM-D, FCM and CLSM techniques. Introduction of QAC into PVDF membrane led to a decrease in hydrophilicity due to the hydrophobic alkyl chains of QAC, a decline in negative zeta potential because of positively charged nitrogen atoms from QAC, and an improvement of average pore sizes. The results showed the modified membranes exhibited clear antibacterial performance. Both the attachment mass and the initial attachment rate of bacteria decreased in the QCM-D tests, indicating that the physiological behavior of antimicrobial QAC dominated the interaction between bacteria and modified membrane surfaces. FCM indicated that cell integrity for the bacteria in the suspension flowing along QAC-modified membrane surfaces was severely affected. CLSM confirmed the significantly lower attachment of total bacteria and higher dead/live cell ratio onto the surface of modified membranes as compared to pristine membranes. Both the FCM and CLSM results verified the bactericidal effects of QAC-modified membrane. The positively charged QAC may attach to the polar surface and then facilitate the penetration of the alkyl chain into the phospholipid bilayer, leading to the death of microbes. Furthermore, the contact-killing effects also lead to the looser attachment of bacteria to membrane surfaces and thus higher reversibility, indicating an excellent antibacterial performance of QAC-modified membranes.

ACKNOWLEDGEMENTS

We gratefully acknowledge the National Natural Science Foundation of China (Grant No. 51678423) for the financial support of the work. This work is also partially supported by State Key Laboratory of Separation Membranes and Membrane Processes (Tianjin Polytechnic University) (Grant M1-201602).

REFERENCES

Blango, M. G. & Mulvey, M. A. 2009 Bacterial landlines: contact-dependent signaling in bacterial populations. *Curr. Opin. Microbiol.* **12** (2), 177–181.

Blok, A. J., Chhasatia, R., Dilag, J. & Ellis, A. V. 2014 Surface initiated polydopamine grafted poly([2-(methacryoyloxy) ethyl]trimethylammonium chloride) coatings to produce reverse osmosis desalination membranes with anti-biofouling properties. *J. Membr. Sci.* **468**, 216–223.

Ceragioli, M., Mols, M., Moezelaar, R., Ghelardi, E., Senesi, S. & Abee, T. 2010 Comparative transcriptomic and phenotypic analysis of the responses of *Bacillus cereus* to various disinfectant treatments. *Appl. Environ. Microbiol.* **76** (10), 3352–3360.

Chen, M., Zhang, X., Wang, Z., Wang, L. & Wu, Z. 2017 QAC modified PVDF membranes: antibiofouling performance, mechanisms, and effects on microbial communities in an MBR treating municipal wastewater. *Water Res.* **120** (Supplement C), 256–264.

Chowdhury, I., Duch, M. C., Mansukhani, N. D., Hersam, M. C. & Bouchard, D. 2014 Deposition and release of graphene oxide nanomaterials using a quartz crystal microbalance. *Environ. Sci. Technol.* **48** (2), 961–969.

Contreras, A. E., Steiner, Z., Miao, J., Kasher, R. & Li, Q. 2011 Studying the role of common membrane surface functionalities on adsorption and cleaning of organic foulants using QCM-D. *Environ. Sci. Technol.* **45** (15), 6309–6315.

Dai, J., Xiao, K., Dong, H., Liao, W., Tang, X., Zhang, Z. & Cai, S. 2016 Preparation of Al2O3/PU/PVDF composite membrane and performance comparison with PVDF membrane, PU/PVDF blending membrane, and Al2O3/PVDF hybrid membrane. *Desalination and Water Treatment* **57** (2), 487–494.

Dolezal, R., Soukup, O., Malinak, D., Savedra, R. M. L., Marek, J., Dolezalova, M., Pasdiorova, M., Salajkova, S., Korabecny, J., Honegr, J., Ramalho, T. C. & Kuca, K. 2016 Towards understanding the mechanism of action of antibacterial N-alkyl-3-hydroxypyridinium salts: biological activities, molecular modeling and QSAR studies. *Eur. J. Med. Chem.* **121**, 699–711.

Dong, H., Xiao, K.-J., Li, X.-L., Ren, Y. & Guo, S.-Y. 2013 Preparation of PVDF/Al2O3 hybrid membrane via the sol–gel process and characterization of the hybrid membrane. *Desalin. Water Treat.* **51**, 3685–3690.

Durmus, N. G., Taylor, E. N., Kummer, K. M. & Webster, T. J. 2013 Enhanced efficacy of superparamagnetic iron oxide nanoparticles against antibiotic-resistant biofilms in the presence of metabolites. *Adv. Mater.* **25** (40), 5706–5713.

Fadida, T., Kroupitski, Y., Peiper, U. M., Bendikov, T., Sela, S. & Poverenov, E. 2014 Air-ozonolysis to generate contact active antimicrobial surfaces: activation of polyethylene and polystyrene followed by covalent graft of quaternary ammonium salts. *Colloid Surface B* **122**, 294–300.

Feng, G., Cheng, Y., Wang, S.-Y., Hsu, L. C., Feliz, Y., Borca-Tasciuc, D. A., Worobo, R. W. & Moraru, C. I. 2014 Alumina surfaces with nanoscale topography reduce attachment and biofilm formation by Escherichia coli and Listeria spp. *Biofouling* **30**, 1253–1268.

Gao, J., Huddleston, N. E., White, E. M., Pant, J., Handa, H. & Locklin, J. 2016 Surface grafted antimicrobial polymer networks with high abrasion resistance. *ACS Biomater. Sci. Eng.* **2**, 1169–1179.

Gerba, C. P. 2015 Quaternary ammonium biocides: efficacy in application. *Appl. Environ. Microbiol.* **81** (2), 464–469.

Gilbert, P. & Moore, L. E. 2005 Cationic antiseptics: diversity of action under a common epithet. *J. Appl. Microbiol.* **99** (4), 703–715.

Goda, T. & Miyahara, Y. 2012 Interpretation of protein adsorption through its intrinsic electric charges: a comparative study using a field-effect transistor, surface plasmon resonance, and quartz crystal microbalance. *Langmuir* **28** (41), 14730–14738.

Gutman, J., Walker, S. L., Freger, V. & Herzberg, M. 2013 Bacterial attachment and viscoelasticity: physicochemical and motility effects analyzed using quartz crystal microbalance with dissipation (QCM-D). *Environ. Sci. Technol.* **47** (1), 398–404.

Habtewold, T., Duchateau, L. & Christophides, G. K. 2016 Flow cytometry analysis of the microbiota associated with the midguts of vector mosquitoes. *Parasites Vectors* **9**, 167.

Harney, M. B., Pant, R. R., Fulmer, P. A. & Wynne, J. H. 2009 Surface self-concentrating amphiphilic quaternary ammonium biocides as coating additives. *ACS Appl Mater Inter.* **1**, 39–41.

Hermansson, M. 1999 The DLVO theory in microbial adhesion. *Colloids and Surfaces B: Biointerfaces* **14** (1–4), 105–119.

Hori, K. & Matsumoto, S. 2010 Bacterial adhesion: from mechanism to control. *Biochem. Eng. J.* **48**, 424–434.

Hu, X., Lin, X., Zhao, H., Chen, Z., Yang, J., Li, F., Liu, C. & Tian, F. 2016 Surface functionalization of polyethersulfone membrane with quaternary ammonium salts for contact-active antibacterial and anti-biofouling properties. *Materials* **9**, 376.

Kang, S.-T., Subramani, A., Hoek, E. M. V., Deshusses, M. A. & Matsumoto, M. R. 2004 Direct observation of biofouling in cross-flow microfiltration: mechanisms of deposition and release. *J. Membr. Sci.* **244** (1–2), 151–165.

Khan, M. M. T., Pyle, B. H. & Camper, A. K. 2010 Specific and rapid enumeration of viable but nonculturable and viable-culturable gram-negative bacteria by using flow cytometry. *Appl. Environ. Microbiol.* **76**, 5088–5096.

Kügler, R., Bouloussa, O. & Rondelez, F. 2005 Evidence of a charge-density threshold for optimum efficiency of biocidal cationic surfaces. *Microbiology* **151**, 1341–1348.

Kuyukina, M. S., Ivshina, I. B., Korshunova, I. O. & Rubtsova, E. V. 2014 Assessment of bacterial resistance to organic solvents using a combined confocal laser scanning and atomic force microscopy (CLSM/AFM). *J. Microbiol. Methods* **107**, 23–29.

Li, Z., Lee, D., Sheng, X., Cohen, R. E. & Rubner, M. F. 2006 Two-level antibacterial coating with both release-killing and contact-killing capabilities. *Langmuir* **22**, 9820–9823.

Li, X., Cai, T., Chen, C. & Chung, T.-S. 2016 Negatively charged hyperbranched polyglycerol grafted membranes for osmotic power generation from municipal wastewater. *Water Res.* **89** (Supplement C), 50–58.

Liu, F., Hashim, N. A., Liu, Y., Abed, M. R. M. & Li, K. 2011 Progress in the production and modification of PVDF membranes. *J. Membr. Sci.* **375**, 1–27.

Liu, Y., Rosenfield, E., Hu, M. & Mi, B. 2013 Direct observation of bacterial deposition on and detachment from nanocomposite membranes embedded with silver nanoparticles. *Water Res.* **47**, 2949–2958.

Liu, X., Jin, X., Cao, B. & Tang, C. Y. 2014 Bactericidal activity of silver nanoparticles in environmentally relevant freshwater matrices: influences of organic matter and chelating agent. *J. Environ. Chem. Eng.* **2**, 525–531.

Lord, M. S., Modin, C., Foss, M., Duch, M., Simmons, A., Pedersen, F. S., Besenbacher, F. & Milthorpe, B. K. 2008 Extracellular matrix remodelling during cell adhesion monitored by the quartz crystal microbalance. *Biomaterials* **29**, 2581–2587.

Lu, N.-Y., Yang, K., Li, J.-L., Yuan, B. & Ma, Y.-Q. 2013 Vesicle deposition and subsequent membrane–melittin interactions on different substrates: a QCM-D experiment. *BBA-Biomembranes* **1828**, 1918–1925.

Makarovsky, I., Boguslavsky, Y., Alesker, M., Lellouche, J., Banin, E. & Lellouche, J.-P. 2011 Novel triclosan-bound hybrid-silica nanoparticles and their enhanced antimicrobial properties. *Adv. Funct. Mater.* **21**, 4295–4304.

Marcus, I. M., Herzberg, M., Walker, S. L. & Freger, V. 2012 *Pseudomonas aeruginosa* attachment on QCM-D Sensors: the role of cell and surface hydrophobicities. *Langmuir* **28**, 6396–6402.

Mollahosseini, A. & Rahimpour, A. 2014 Interfacially polymerized thin film nanofiltration membranes on TiO2 coated polysulfone substrate. *J. Industr. Eng. Chem.* **20**, 1261–1268.

Oh, H.-S., Yeon, K.-M., Yang, C.-S., Kim, S.-R., Lee, C.-H., Park, S. Y., Han, J. Y. & Lee, J.-K. 2012 Control of membrane biofouling in mbr for wastewater treatment by quorum quenching bacteria encapsulated in microporous membrane. *Environ. Sci. Technol.* **46**, 4877–4884.

Olofsson, A.-C., Hermansson, M. & Elwing, H. 2005 Use of a Quartz crystal microbalance to investigate the antiadhesive potential of N-acetyl-l-cysteine. *Appl. Environ. Microbiol.* **71**, 2705–2712.

Olsson, A. L. J., van der Mei, H. C., Busscher, H. J. & Sharma, P. K. 2010 Novel analysis of bacterium-substratum bond maturation measured using a quartz crystal microbalance. *Langmuir* **26**, 11113–11117.

Olsson, A. L. J., Mitzel, M. R. & Tufenkji, N. 2015 QCM-D for non-destructive real-time assessment of Pseudomonas aeruginosa biofilm attachment to the substratum during biofilm growth. *Colloids Surf.* **136**, 928–934.

Pembrey, R. S., Marshall, K. C. & Schneider, R. P. 1999 Cell surface analysis techniques: what do cell preparation protocols do to cell surface properties? *Appl. Environ. Microbiol.* **65**, 2877–2894.

Perreault, F., Tousley, M. E. & Elimelech, M. 2014 Thin-film composite polyamide membranes functionalized with biocidal graphene oxide nanosheets. *Environ. Sci. Technol. Lett.* **1**, 71–76.

Pires, L., Sachsenheimer, K., Kleintschek, T., Waldbaur, A., Schwartz, T. & Rapp, B. E. 2013 Online monitoring of biofilm growth and activity using a combined multi-channel impedimetric and amperometric sensor. *Biosens. Bioelectron.* **47**, 157–163.

Qi, S., Li, Y., Zhao, Y., Li, W. & Tang, C. Y. 2015 Highly efficient forward osmosis based on porous membranes-applications and implications. *Environ. Sci. Technol.* **49**, 4690–4695.

Rahaman, M. S., Therien-Aubin, H., Ben-Sasson, M., Ober, C. K., Nielsen, M. & Elimelech, M. 2014 Control of biofouling on reverse osmosis polyamide membranes modified with biocidal nanoparticles and antifouling polymer brushes. *J. Mater. Chem. B* **2** (12), 1724–1732.

Ronen, A., Duan, W., Wheeldon, I., Walker, S. & Jassby, D. 2015 Microbial attachment inhibition through low-voltage electrochemical reactions on electrically conducting membranes. *Environ. Sci. Technol.* **49**, 12741–12750.

Schofield, A. L., Rudd, T. R., Martin, D. S., Fernig, D. G. & Edwards, C. 2007 Real-time monitoring of the development and stability of biofilms of *Streptococcus mutans* using the quartz crystal microbalance with dissipation monitoring. *Biosens. Bioelectron.* **23** (3), 407–413.

Shannon, M. A., Bohn, P. W., Elimelech, M., Georgiadis, J. G., Marinas, B. J. & Mayes, A. M. 2008 Science and technology for water purification in the coming decades. *Nature* **452**, 301–310.

Tagaya, M., Ikoma, T., Takemura, T., Hanagata, N., Okuda, M., Yoshioka, T. & Tanaka, J. 2011 Detection of interfacial phenomena with osteoblast-like cell adhesion on hydroxyapatite and oxidized polystyrene by the quartz crystal microbalance with dissipation. *Langmuir* **27**, 7635–7644.

Tezel, U. & Pavlostathis, S. G. 2011 Role of quaternary ammonium compounds on antimicrobial resistance in the environment. antimicrobial resistance in the environment. In: *Antimicrobial Resistance in the Environment* (P. L. Keen & M. H. M. M. Montforts, eds). John Wiley & Sons, Inc., Hoboken, NJ, USA, pp. 349–387.

Tezel, U. & Pavlostathis, S. G. 2015 Quaternary ammonium disinfectants: microbial adaptation, degradation and ecology. *Curr. Opin. Biotechnol.* **33**, 296–304.

Thwala, J. M., Li, M., Wong, M. C. Y., Kang, S., Hoek, E. M. V. & Mamba, B. B. 2013 Bacteria–polymeric membrane interactions: atomic force microscopy and XDLVO predictions. *Langmuir* **29**, 13773–13782.

Tiraferri, A., Kang, Y., Giannelis, E. P. & Elimelech, M. 2012 Highly hydrophilic thin-film composite forward osmosis membranes functionalized with surface-tailored nanoparticles. *ACS Appl. Mater. Interfaces* **4**, 5044–5053.

Vadillo-Rodríguez, V. & Logan, B. E. 2006 Localized attraction correlates with bacterial adhesion to glass and metal oxide substrata. *Environ. Sci. Technol.* **40**, 2983–2988.

Vanoyan, N., Walker, S. L., Gillor, O. & Herzberg, M. 2010 Reduced bacterial deposition and attachment by quorum-sensing inhibitor 4-nitro-pyridine-N-oxide: the role of physicochemical effects. *Langmuir* **26**, 12089–12094.

Venault, A., Liu, Y.-H., Wu, J.-R., Yang, H.-S., Chang, Y., Lai, J.-Y. & Aimar, P. 2014 Low-biofouling membranes prepared by liquid-induced phase separation of the PVDF/polystyrene-b-poly (ethylene glycol) methacrylate blend. *J. Membr. Sci.* **450**, 340–350.

Venault, A., Huang, W.-Y., Hsiao, S.-W., Chinnathambi, A., Alharbi, S. A., Chen, H., Zheng, J. & Chang, Y. 2016 Zwitterionic modifications for enhancing the antifouling properties of poly(vinylidene fluoride) membranes. *Langmuir* **32**, 4113–4124.

Wadekar, S. S. & Vidic, R. D. 2017 Influence of active layer on separation potentials of nanofiltration membranes for inorganic ions. *Environ. Sci. Technol.* **51**, 5658–5665.

Wang, J., Wang, Z., Liu, Y., Wang, J. & Wang, S. 2016 Surface modification of NF membrane with zwitterionic polymer to improve anti-biofouling property. *J. Membr. Sci.* **514**, 407–417.

Yang, Z., Wu, Y., Wang, J., Cao, B. & Tang, C. Y. 2016 In situ reduction of silver by polydopamine: a novel antimicrobial

modification of a thin-film composite polyamide membrane. *Environ. Sci. Technol.* **50**, 9543–9550.

Ye, G., Lee, J., Perreault, F. & Elimelech, M. 2015 Controlled architecture of dual-functional block copolymer brushes on thin-film composite membranes for integrated 'defending' and 'attacking' strategies against biofouling. *ACS Appl. Mater. Interfaces* **7**, 23069–23079.

Zhang, T., Zhu, C., Ma, H., Li, R., Dong, B., Liu, Y. & Li, S. 2014 Surface modification of APA-TFC membrane with quaternary ammonium cation and salicylaldehyde to improve performance. *J. Membr. Sci.* **457**, 88–94.

Zhang, J., Wang, Z., Zhang, X., Zheng, X. & Wu, Z. 2015a Enhanced antifouling behaviours of polyvinylidene fluoride membrane modified through blending with nano-TiO2/ polyethylene glycol mixture. *Appl. Surf. Sci.* **345**, 418–427.

Zhang, S., Bai, H., Pi, J., Yang, P. & Cai, J. 2015b Label-free quartz crystal microbalance with dissipation monitoring of resveratrol effect on mechanical changes and folate receptor expression levels of living MCF-7 cells: a model for screening of drugs. *Anal. Chem.* **87**, 4797–4805.

Zhang, X., Ma, J., Tang, C. Y., Wang, Z., Ng, H. Y. & Wu, Z. 2016a Antibiofouling polyvinylidene fluoride membrane modified by quaternary ammonium compound: direct contact-killing versus induced indirect contact-killing. *Environ. Sci. Technol.* **50**, 5086–5093.

Zhang, X., Wang, Z., Chen, M., Liu, M. & Wu, Z. 2016b Polyvinylidene fluoride membrane blended with quaternary ammonium compound for enhancing anti-biofouling properties: effects of dosage. *J. Membr. Sci.* **520**, 66–75.

Zhu, Y., Xie, W., Zhang, F., Xing, T. & Jin, J. 2017 Superhydrophilic in-situ-cross-linked zwitterionic polyelectrolyte/pvdf-blend membrane for highly efficient oil/water emulsion separation. *ACS Appl. Mater. Interfaces* **9**, 9603–9613.

First received 3 April 2018; accepted in revised form 28 April 2018. Available online 31 May 2018